Preparation and characterization of carbon-terminated β-SiC(001) surfaces

V. M. Bermudez and R. Kaplan
Naval Research Laboratory, Washington, D.C. 20375-5000
(Received 1 March 1991)

Carbon-terminated surfaces have been formed on the initially Si-terminated β-SiC(001)-(2×1) surface by exposure to C_2H_4 at 800 °C–1100 °C. The structure of these surfaces (both as formed and after atomic-H adsorption) has been investigated using Auger and electron-energy-loss spectroscopies, low-energy electron diffraction, and electron-stimulated desorption of H^+. A model is proposed for the $c(2\times2)$ ordered C monolayer consisting of sp^3 single-bonded C—C units with each C bridging two nearest-neighbor Si atoms. These species exhibit a high degree of thermal stability, and the single dangling bond remaining on each C is an active site for the thermally reversible adsorption of atomic H. This $c(2\times2)$ surface is shown to be essentially the same as that formed by thermal desorption of Si from the (2×1) surface but is more uniform and well ordered.

INTRODUCTION

The surface properties of hexagonal α- and cubic β-SiC and the formation of oxides and metal interfaces on these materials have received much attention recently. This has been motivated in part by the obvious relevance of such information to the fabrication of SiC-based electronic devices. Furthermore, β-SiC is of fundamental interest in that it serves as a bridge between the column IV elemental semiconductors Si and Ge and the III-V compound materials such as GaAs. Detailed studies[1] of the β-SiC(001) and β-SiC(111) surface reconstructions for different stoichiometries have been reported and comparison made with Si and Ge surface structures.

For β-SiC(001), much work to date has focused on the stoichiometric Si-terminated (2×1) and Si-rich (3×2) surfaces described in Ref. 1. A Si-deficient (i.e., C-rich) $c(2\times2)$ surface can also be prepared by annealing the (2×1) surface at ≥ 1200 °C in ultrahigh vacuum (UHV). This surface is relatively inert to room temperature adsorption of O_2, in contrast to Si and to other SiC surfaces,[2] and forms sharp interfaces at room temperature with metals such as Ti (Ref. 3) and Ni.[4] Yet the $c(2\times2)$ structure is not understood, and LEED (Ref. 1) (low-energy electron diffraction), STM (Ref. 5) (scanning tunneling microscopy) and MEIS (Ref. 6) (medium-energy ion scattering) results to date are ambiguous as to the exact nature of the reconstruction.

A difficulty in any systematic study of this Si-deficient surface is that, as a result of the method of preparation, it is intrinsically inhomogeneous and probably contains a high density of defects. The transitions from (3×2) to (2×1) to $c(2\times2)$ to the graphitelike (1×1) phase[1] with increasing annealing temperature are not sharp. Thus electron energy loss[1] (ELS) and valence-band photoemission[2] spectra of one surface phase frequently show weak features associated with other phases. Attempts to prepare the $c(2\times2)$ surface at lower temperature, to avoid the (1×1) phase, almost always result in residual (2×1) patches. The present work was motivated by an interest in preparing homogeneous and well-characterized C-terminated surfaces by adsorption of excess C on, rather than desorption of Si from, an initially stoichiometric surface. The approach is analogous to the preparation of the (3×2) structure by adsorption of excess Si. Recent theoretical work[7] has suggested that a C-terminated surface could be stabilized by C-dimer pairing.

In the present work, C-terminated surfaces are formed by reaction of the SiC(001)-(2×1) surface with ethylene (C_2H_4) at elevated temperatures and are studied using a variety of techniques. LEED and Auger electron spectroscopy (AES), with particular attention to line shapes, are used to monitor surface composition and order. ELS in the valence, Si 2*p*, and C 1*s* excitation regions is used as a probe of structure-related changes in bonding. The reaction of the C-terminated surface with atomic H is investigated and provides further insight into the surface structure. Electron stimulated desorption (ESD) of H^+ is used as a means of directly detecting adsorbed H. Finally, some results are also reported for the reaction of the (001)-(2×1) surface with methane (CH_4) and for reaction of the (001)-(3×2) with C_2H_4.

EXPERIMENTAL DETAILS

The samples were SiC(001) films, about 5 μm thick, grown on Si(001) substrates oriented from 0.5° to 4° off (001) in the (110) direction. The resulting clean SiC surfaces exhibit a single (2×1) or $c(4\times2)$ domain in LEED, whereas, those for on-axis substrates show two orthogonal domains.[1,8] For ESD, on-axis samples were used as a result of sample availability and the particular requirements as to sample configuration imposed by the experiment. Other than the clean-surface LEED characteristics, no difference was observed between on- and off-axis samples. The preparation and characterization of clean surfaces have been described in detail previously.[1,2,9]

The (2×1) surface was exposed to C_2H_4 (nominally

99.5% pure) at substrate temperatures as high as 1100 °C. The upper limit was chosen to be well below the temperature (≈1200 °C) at which Si desorption becomes significant on the time scale of a typical series of exposures. Exposures ranged from 10 to 2×10^3 L [1 langmuir (L)$\equiv10^{-6}$ Torr sec] based on uncorrected nude ionization gauge pressure values. During exposure the C_2H_4 flowed through the chamber at pressures of from 2×10^{-7} to 5×10^{-6} Torr, depending on the desired exposure, with continuous ion pumping. Unless otherwise noted, no impurities were detected above the AES elemental sensitivity limits. Some experiments were also performed using methane (CH_4, 99.99% pure). For exposure to atomic H, the chamber was dynamically backfilled with H_2 while the sample faced a W filament, resistively heated to about 1700 °C, at a distance of about 3 cm. The resulting flux of H is not known accurately, and exposures are quoted in terms of the uncorrected H_2 ionization gauge pressure readings. Such H_2 exposures will be referred to as "filament-assisted."

Auger and ELS data were obtained using a cylindrical mirror analyzer with the coaxial electron beam incident normal to the sample surface. For AES surveys, a primary beam of $E_p=3$ keV and $i_p\approx3.5$ μA was used with a peak-to-peak modulation of $\delta E=2$ eV. A δE of 1 eV was used for scans of the Si LVV and C KLL fine structure. For ELS in the regions of valence, Si $2p$ and C $1s$ excitation, E_p's of approximately 96, 240, and 420 eV, respectively, were used with a $\delta E=0.5$ eV (unless otherwise noted). These values of E_p gave nearly optimum surface sensitivity (i.e., loss features in the 70–140-eV kinetic-energy range) while maintaining the core excitation losses well above the strong 88-eV Si LVV peak. The net resolution in ELS (full width at half maximum of a 100-eV elastic peak) was 0.7–0.8 eV for $\delta E=0.5$ eV. The ELS data were recorded in the first-derivative ($d[EN(E)]/dE$) form and, to aid in peak location, could be numerically differentiated to give spectra in the $-d^2[EN(E)]/dE^2$ form. The data were checked for evidence of damage by the Auger and ELS primary beams by repeatedly scanning the same spot on the sample surface and by comparing such spectra with those for previously unirradiated spots. Except for slow ESD of H after exposure of the C-terminated surface to atomic H, there was no indication of beam-induced changes in fine structure or line shapes in any of the spectra. Except where noted, all data were recorded with the sample at nominal room temperature.

H^+ ESD data were obtained as described previously[10] using a computer-controlled electron gun (beam energy and focus) giving $0<E_p<100$ eV and $i_p\approx0.55$ μA. The electron energy was referenced to the Fermi level (E_F) by adding the work function ($\phi_c=4.1$ eV) and thermal energy ($kT_c\approx0.2$ eV) of the Ta cathode and the spectrum (ion yield versus $E_p+\phi_c+kT_c$) corrected for the energy dependence of i_p. The kinetic-energy distribution of the desorbed ions (IED) was determined using a retarding potential technique, similar to that described by Bozack *et al.*,[11] in which a variable bias (V_R) is applied between the sample and ground and the ion yield recorded versus V_R at fixed E_p.

RESULTS AND DISCUSSION

A. LEED patterns and Auger intensities

Figures 1–3 show LEED and Auger data for various surface phases. The clean SiC surface shows the single-domain (2×1) LEED pattern and Si LVV and C KLL line shapes discussed earlier.[1] The I(C(268 eV))/I(Si(88 eV)) peak-to-peak height (PPH) ratio is about 0.27, as before.[1] Figure 4 shows the I(C)/I(Si) PPH ratio versus C_2H_4 exposure at 1100 °C, labeled to indicate the ranges within which various LEED patterns are observed.

Stepwise exposure to C_2H_4 at 1100 °C leads to a steady increase in C coverage which reaches quasisaturation at about 70 L with an I(C)/I(Si) PPH ratio ≈0.82. The original (2×1) LEED pattern (Fig. 1) is first replaced by a (1×2) pattern with weak and diffuse fractional-order spots. At about 50 L [I(C)/I(Si) PPH ratio ≈0.64], this pattern begins giving way to a $c(2\times2)$ structure. There are subtle changes in the Si LVV and C KLL line shapes, relative to the clean (2×1) surface, and the main Si peak shifts from 88 to 85 eV for the $c(2\times2)$. The (1×2) surface shows evidence of both the shifted and unshifted peaks. Heating the $c(2\times2)$ surface at 1200 °C–1250 °C in UHV for a few minutes causes a return of the weak (1×2) LEED pattern with no change (i.e., less than a few percent) in the I(C)/I(Si) PPH ratio. The (1×2) fractional-order LEED spots are never as sharp or bright as those of the (2×1) and $c(2\times2)$ surfaces. Below the $c(2\times2)\rightarrow(1\times2)$ conversion temperature, the $c(2\times2)$ structure is quite stable in that the LEED pattern can be seen with the sample maintained as high as 1000 °C. This is facilitated by the high β-SiC Debye temperature [$\Theta_D\approx1000$ °C (Ref. 12)]. Above this temperature, the

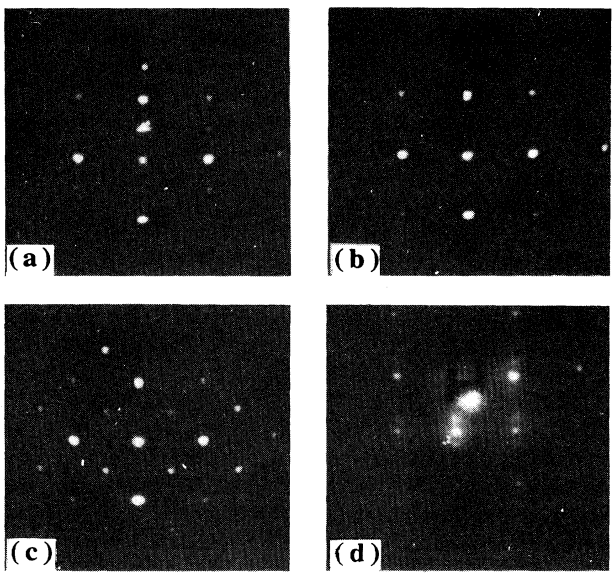

FIG. 1. LEED patterns for (a) (2×1), (b) (1×2), (c) $c(2\times2)$, and (d) (1×1) single-domain β-SiC(001) surfaces. Data were obtained at a primary beam energy of 99 eV except for the (1×1) which was obtained at 116 eV.

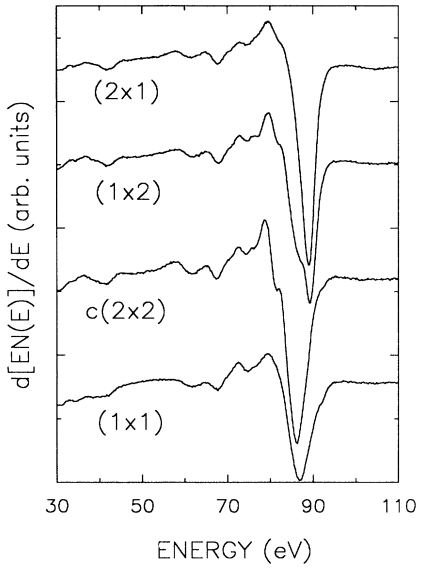

FIG. 2. Si *LVV* spectra for the (2×1), (1×2), $c(2\times2)$, and (1×1) SiC(001) surfaces. The relative magnitudes of different spectra are not quantitative.

pattern is obscured by light emitted by the hot sample.

Much larger exposures at 1100 °C lead to a further small increase in the I(C)/I(Si) PPH ratio and changes in the Si *LVV* and C *KLL* line shapes. Subtracting the $c(2\times2)$ C *KLL* spectrum shows that the change in this region results from the superposition of a graphite C line

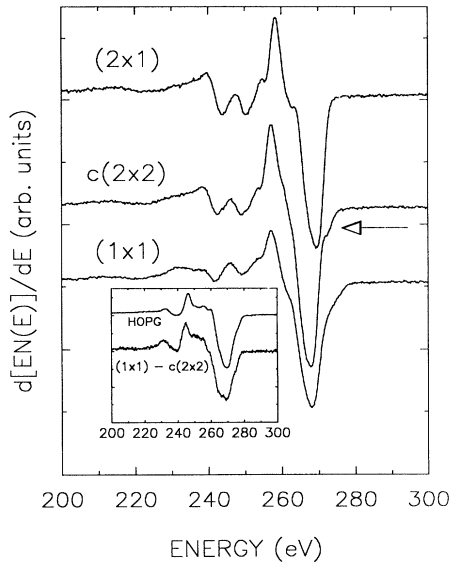

FIG. 3. Same as Fig. 2 but showing the C *KLL* data. The inset shows the (1×1)-$c(2\times2)$ C *KLL* difference spectrum compared to that for highly oriented pyrolytic graphite (HOPG). The difference spectrum is computed by scaling and shifting the $c(2\times2)$ spectrum to minimize the upward-pointing peak at 258 eV in the (1×1)-$c(2\times2)$ difference. The feature indicated by the arrow corresponds to a final state involving a dangling C bond (see text).

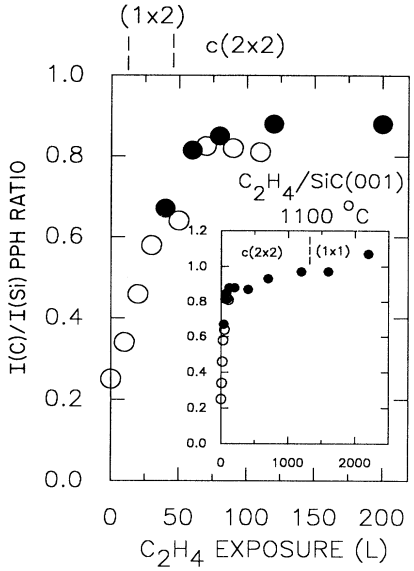

FIG. 4. I(C(268 eV))/I(Si(88 eV)) peak-to-peak height (PPH) ratio vs C_2H_4 exposure at 1100 °C, beginning with the Si-terminated SiC(001)-(2×1) surface. Approximate regions are delineated in which the different LEED patterns are observed. The open and solid circles indicate data taken in different runs.

shape. The PPH of the difference spectrum indicates that about one-third of the total C *KLL* signal arises from graphitic C. At the same time, the fractional-order LEED spots decrease in brightness, and the $c(2\times2)$ pattern is gradually replaced by a (1×1). Coincident with the (1×1) is a weak pattern suggestive of an incommensurate ordered overlayer with, however, no indication of features related to polycrystalline graphite (e.g., diffraction rings, as in Ref. 9).

On the basis of the MEIS results of Hara *et al.*,[6] the coverage of adsorbed C at the quasisaturation point ($\approx$70 L, Fig. 4) is estimated to be one monolayer. These authors compared the relative intensities of the Si and C ion backscatter peaks for the thermally generated $c(2\times2)$ structure and concluded that the surface is terminated by a full monolayer of C. As discussed below, we obtain nearly the same I(C)/I(Si) PPH ratios for this surface and for the C_2H_4-derived $c(2\times2)$, and other observations indicate that the two surfaces are the same except that the latter is more homogeneous and well ordered.

Within experimental uncertainty, exposures of $\leq$200 L at 800 °C gave the same results as those at 1100 °C shown in Fig. 4. A finite adsorption probability was found at room temperature, for which a 50-L exposure gave a small increase in the I(C)/I(Si) PPH ratio; however, the initial reaction rate slows appreciably below about 500 °C.

A series of C_2H_4 exposures at 1000 °C was performed starting with a (3×2) surface. This surface consists[1] of a two-thirds monolayer of excess Si adsorbed on the Si termination layer of the (2×1) surface. Si-Si dimer pairing occurs within this excess Si layer as on the (2×1) surface.

For exposures of up to 200 L, no change in LEED pattern was observed, and the $I(C)/I(Si)$ Auger ratio remained constant to within 10%. Although the meaning of this null result is not clear at present, it is consistent with previous data[2] for the exposure of SiC(001) to O_2. These show a much slower initial rate of O uptake for the (3×2) surface which was tentatively interpreted in terms of a stronger Si-Si dimer interaction than on the (2×1) surface.

Reaction of the (2×1) surface with CH_4 is much slower than with C_2H_4. A series of CH_4 exposures at 1100 °C, up to a total of 500 L, led to a gradual increase in the $I(C)/I(Si)$ PPH ratio by only about 40% (cf. Fig. 4). A clear (2×1) LEED pattern remained; however, beam intensities versus E_p were not recorded, so it is unknown whether the resulting structure differs from that of the clean surface.

B. Auger line shapes

The 3-eV shift to lower energy of the main Si $L_{2,3}VV$ peak (Fig. 2) can be understood in terms of changes in the valence-band density of states (VB DOS) as revealed in photoemission spectra.[2] For elemental Si, the VB DOS can be separated into mainly $3s$ and mainly $3p$ components and the $L_{2,3}VV$ spectrum[13] represented as a self-convolution of the form $(s+p)*(s+p)$, weighted by matrix elements appropriate to the different two-hole final states $s*s$, $s*p$, and $p*p$ (where $*$ indicates the convolution operation). The matrix element is largest, and the DOS greatest, for $p*p$ which gives rise to the strong negative maximum at 88 eV in $d[EN(E)]/dE$. This final state places both holes mainly in Si $3p$ orbitals in the DOS peak near the VB maximum; hence, a shift of δE to higher binding energy on the part of this peak will be reflected in the Si $L_{2,3}VV$ spectrum as a shift of $2(\delta E)$ to lower kinetic energy, assuming a constant final-state hole-hole interaction.[13] Photoemission data[2] indeed show a shift of about 2 eV to higher binding energy for the VB DOS peak on going from the (2×1) to the $c(2\times2)$ surface. Furthermore, close inspection of the weak Si $L_1L_{2,3}V$ peak near 40 eV (Fig. 2) also reveals a small shift to lower energy on going from (2×1) to $c(2\times2)$.

The C KLL spectrum for the $c(2\times2)$ surface (Fig. 3) shows a weak shoulder, on the high-energy side of the main peak, at about 272 eV. This feature is also seen for the (1×2) surface (not shown) and for the (1×1) but not the (2×1). Growth of a similar structure has been observed during the thermal desorption of H from amorphous carbon films.[14] We interpret this feature in terms of an Auger transition in which one of the two electrons involved in the core hole decay is derived from a C dangling-bond orbital. Other data (see below) will provide independent evidence of the occurrence of C dangling bonds on the $c(2\times2)$ surface. It is unclear at present whether this dangling bond orbital is occupied in the electronic ground state or becomes occupied as a result of a resonant C $1s$ excitation (the "ke-v" Auger process described by Ramaker[15]). However, the absence of band-gap states in the $c(2\times2)$ photoemission spectrum[2] argues against the former. Comparison of x-ray- and electron-excited C KLL line shapes would be useful in clarifying this point.[15]

C. ELS

Figure 5 shows the surface-sensitive ELS data for plasmon and valence excitations, and Figs. 6 and 7 give corresponding results for C $1s$ and Si $2p$ excitations, respectively.

1. *Valence and plasmon excitation*

The low-energy loss spectrum (Fig. 5) for the (2×1) surface is in good agreement with previous results.[1,2] Exposure to C_2H_4 to form the (1×2) surface has an effect on the (2×1) similar to that of the initial adsorption of oxygen.[2] The surface state transitions[2] at about 2 eV (in this case a poorly resolved shoulder) and at about 5 eV are eliminated. In addition the peak at about 12 eV is attenuated. The (1×1) spectrum shows a pronounced peak at about 7 eV characteristic[16,17] of the π plasmon excitation in graphite.

2. *C 1s excitation*

Significant differences in the C $1s$ ELS are seen for the various surface phases (Fig. 6). Similar data have been obtained previously for different forms of pure C using ELS (Refs. 17–19) and soft x-ray absorption.[20,21] The shape of the (2×1) ELS resembles that of diamond,[18,19] with a broad peak at about 285 eV and a weaker feature near 300 eV, indicating σ-bonded sp^3-hybridized C. The transition energies for SiC are about 5 eV lower than for

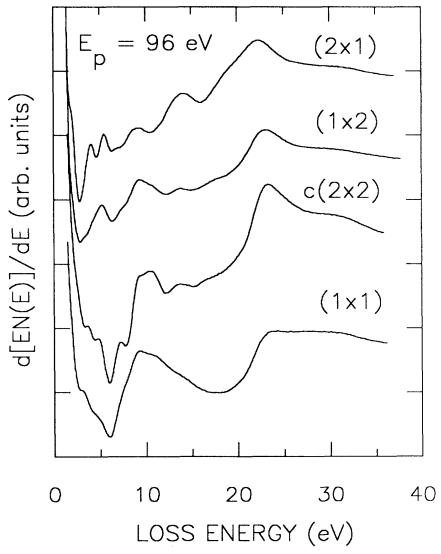

FIG. 5. ELS results in the region of plasmon and valence excitations for the (2×1), (1×2), $c(2\times2)$, and (1×1) surfaces. The primary beam energy was 96 eV and the resolution 0.7 eV. The relative magnitudes of different spectra are not quantitative. The loss energies quoted in the text refer to inflection points in the first-derivative spectra.

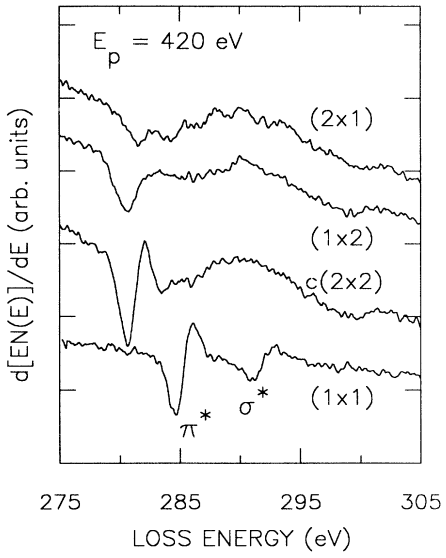

FIG. 6. ELS for C 1*s* excitation for the (2×1), (1×2), $c(2\times2)$, and (1×1) surfaces. The primary beam energy was 420 eV and the resolution 0.8 eV. π^* and σ^* indicate the graphitic conduction-band final states assigned to the (1×1) loss peaks (see text).

diamond,[18,19] reflecting the smaller bandgap of SiC (2.4 versus 5.5 eV) and the approximately 1.4-eV smaller C 1*s* binding energy.[22] As in the case of diamond,[18] other structure is observed between the two main loss peaks; however, these features are very weak and not entirely reproducible. At the other extreme, the (1×1) surface shows relatively sharp peaks at 285.5 and 292.0 eV. Peaks at these same energies are found[17,18] for graphite and glassy C where they are assigned to C $1s\rightarrow\pi^*$ and C $1s\rightarrow\sigma^*$ transitions, respectively. Note that the (1×1) spectrum, unlike that of the $c(2\times2)$, shows no evidence of the 285- and 300-eV bands seen for the (2×1) surface, even though the adsorbed C coverage is not much higher than for the $c(2\times2)$ (Fig. 4). This suggests that the substrate Si-C backbonds are substantially affected by the formation of the (1×1) phase.

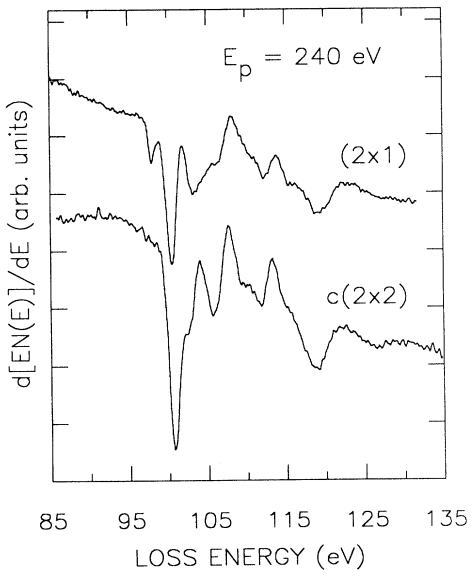

FIG. 7. ELS for Si 2*p* excitation for the (2×1) and $c(2\times2)$ surfaces. The primary beam energy was 240 eV and the resolution 0.8 eV.

For the (1×2) surface, a sharp peak resembling the graphite π^* (but no feature similar to the σ^*) appears at 281.5 eV superimposed on the original (2×1) loss structure. On forming the $c(2\times2)$, this peak becomes more intense and symmetric. These results indicate a second form of carbon coexisting with that originally present. The growth of this loss peak parallels that of similar structures, during thermal desorption of H, in the diamond (111) ELS (Ref. 19) (at 284 eV) and in the near-edge absorption spectrum[20] of amorphous C (at 283.5 eV). H desorption in these materials[19,20] leads to threefold-coordinated C sites, and H effects on the $c(2\times2)$ surface will be discussed below. Spectra of the $c(2\times2)$ surface recorded at sample temperatures as high as 1100 °C continue to show this sharp loss peak, indicating a high degree of thermal stability for the adsorbed C structure.

The C 1*s* ELS data, together with the high-energy C *KLL* satellite discussed above, suggest the presence of C dangling bonds on the $c(2\times2)$ surface. If the (1×1) spectrum in Fig. 6 is taken as characteristic of sp^2-hybridized and π-bonded C, then the $c(2\times2)$ spectrum implies C which is not fourfold coordinated but not π-bonded either.

For SiC(001)–(2×1), a bulk C 1*s* binding energy of 282.7 eV below E_F was reported,[23] using Mg $K\alpha$ excitation, for *n*-type samples similar to those employed in the present study. This is about 1.2 eV greater than the 281.5-eV loss energy of the sharp $c(2\times2)$ peak. Tl is discrepancy can be explained largely in terms of an initial-state effect if the ELS transition involves a C dangling bond. For clean diamond (111), highly surface-sensitive photoemission spectra[24,25] show a C 1*s* level shifted about 0.85 eV to lower binding energy relative to that of the bulk C. Since this feature is removed by H adsorption, the shift almost certainly arises from the presence of sp^3 dangling bonds on the clean surface. Similar photoemission data with the required resolution and surface sensitivity are not yet available for SiC. The remaining $\approx$0.35 eV required to place the ELS final state at or above E_F could be derived from a finite C 1*s* exciton binding energy (reported[26] to be 0.19 eV for diamond) and/or from a further shift of the adsorbed C 1*s* relative to that of the substrate C.

3. *Si 2p excitation*

Si 2*p* ELS data for the (2×1) and $c(2\times2)$ surfaces are shown in Fig. 7. The results agree with those of Dayan[27] obtained at somewhat lower resolution. The SiC(001)-(2×1) Si 2*p* binding energy[23] is 99.9 eV below E_F (for *n*-type samples similar to those used here). Hence, the major loss peak at about 101.5 eV corresponds to a final state just above the bottom of the conduction band,

where a Si-derived peak occurs[28] in the β-SiC DOS. The (2×1) surface also shows a peak at about 98.5 eV which might involve a surface exciton. However, this peak is more likely associated with small residual patches of excess Si (as discussed above) since the major $2p$ ELS peak[29] for elemental Si [the (001)-(2×1) surface] is at 98.7 eV. In any case, the absence of a similar feature in the $c(2\times2)$ spectrum suggests the absence of Si-derived surface states (particularly Si dangling bonds) in the band gap for this surface.

D. Adsorption of atomic H on the $c(2\times2)$ surface

Further insight into the $c(2\times2)$ structure can be gained from examination of the effects of atomic H on this surface. Figures 8 and 9 show Auger and ELS data for a 300-L filament-assisted H_2 exposure (as described above). LEED continues to show a $c(2\times2)$ pattern with, however, current-voltage (I-V) characteristics different from those of the original $c(2\times2)$. For example, the H-exposed surface shows bright and sharp fractional-order spots at $E_p \approx 50$ eV; whereas, these are barely detectable by eye at 50 eV for the original $c(2\times2)$. H adsorption also causes a small ($\approx 15\%$) decrease in the I(C)/I(Si) PPH ratio. These effects are reversed by annealing for 1 min at 1100 °C to desorb the H. Henceforth, the H-exposed $c(2\times2)$ surface is labeled "SiC(001)-$c(2\times2)$H" or simply "$c(2\times2)$H" with the adsorbed C layer being implicit in the "$c(2\times2)$" designation. After atomic H exposure, a small impurity O signal was often detected in Auger, but there was no correlation between the O coverage and any of the H effects reported here.

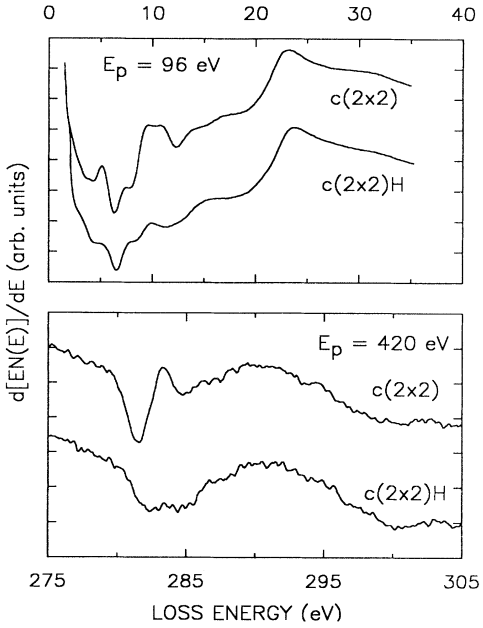

FIG. 9. ELS data in the regions of valence and plasmon excitation (upper) and C 1s excitation (lower) for the $c(2\times2)$ surface before and after H adsorption. All changes caused by H adsorption are reversed when H is thermally desorbed. For both C 1s spectra, the resolution was degraded to about 2 eV to reduce the required signal averaging time (see text).

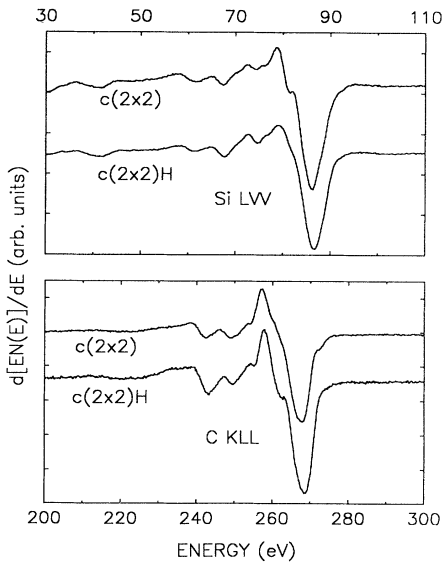

FIG. 8. Si LVV (upper) and C KLL (lower) spectra for the $c(2\times2)$ surface before and after atomic H adsorption, the latter surface being designated "$c(2\times2)$H" (see text). The relative magnitudes of different spectra are not quantitative. All changes caused by H adsorption are reversed when H is thermally desorbed. Note in particular the removal by H of the C KLL dangling-bond satellite (cf. Fig. 3).

H adsorption causes subtle changes in the Si and C Auger lineshapes (Fig. 8) and more substantial effects in the low-energy and C 1s ELS data (Fig. 9). Both C 1s spectra were obtained with the modulation increased to 2 eV (from the usual value of 0.5 eV) to reduce the required signal averaging and, thereby, the slow ESD of H by the ELS primary beam. Both sets of ELS data show primarily structure being removed by H adsorption with no obvious new features being introduced. These changes are also completely reversible upon desorption of H at 1100 °C. Of particular significance is the H-induced disappearance of the dangling-bond features from the C 1s ELS and the C KLL AES. On the other hand, no H effects were noticeable in the Si 2p ELS (not shown), suggesting that H adsorbed on the $c(2\times2)$ surface bonds only to C and that Si dangling bonds are not a characteristic of this surface.

The existence of the $c(2\times2)$H structure has certain interesting implications. H saturation removes C dangling bonds but does not remove the surface reconstruction to give a (1×1)H LEED pattern as is the case for, e.g., the (001)-(2×1) surface. This indicates that the $c(2\times2)$ structure on the H-free surface arises from actual chemical bonding rather than from a weaker dangling-bond di-

mer pairing. While the existence of such a dangling-bond interaction cannot be ruled out, it is clearly not the major effect stabilizing the $c(2\times2)$ structure. The small change in I-V characteristics with H adsorption, however, further suggests that H induces some relaxation of the distances and/or angles of these chemical bonds.

E. ESD

Figure 10 shows ESD results for the $c(2\times2)$H surface. In addition to H^+, ions were detected at masses 16 (O^+) and 19 (F^+). A very weak signal was also observed at mass 17 (^+OH), but no other species were seen. The presence of O^+ and F^+, even though neither was detected in Auger spectra, parallels earlier ESD results for α-SiC (Ref. 10) and Si(001) (Ref. 11). Most ion signals were eliminated by a few volts negative bias on the sample, indicating that the ESD arises from the sample and not from scattered electrons striking metals parts at the entrance to the mass spectrometer. However, for E_p well above threshold, this process was found to yield a significant spurious H^+ signal which persisted after thermal desorption of H from the sample.

The threshold electron energy for H^+ ESD was 22 ± 1 eV, in good agreement with the value of 21 ± 1 eV for both the Si- and C-terminated α-SiC(0001) surfaces.[10] The O^+ threshold was 35 ± 1 eV versus 33 ± 1 eV for the α-SiC C face. However, the F^+ threshold of 30 eV was about 6 eV higher than for C-terminated α-SiC. The H^+ IED peaks near $V_R\approx0$ (uncorrected for the difference between the vacuum levels of the sample and mass spectrometer). As a check, IED's were also measured for O^+ and F^+ (not shown). O and F are more electronegative than H, i.e., more negatively charged in the electronic ground state. Hence, a more energetic "Coulomb explosion" should result when electronic excitation "suddenly" (i.e., nonadiabatically) converts these species to positive ions. In agreement with this simple argument, the O^+ and F^+ IED's peak at $V_R\approx-5.2$ and -1.8 V, respectively. The meaning of an H^+ IED extending up to $V_R\approx+3$ V ("negative kinetic energy") is that the vacuum-level cutoff of the spectrometer lies higher than that of the sample. Arbitrarily shifting the IED by -3 V would place the peak at about -2.5 V, in good agreement with H^+ energies (≈2–3 eV) observed for H/Si(001) (Ref. 30), solid $(CH_3)_4C$ (Ref. 31) and H/GaAs(001) (Ref. 32).

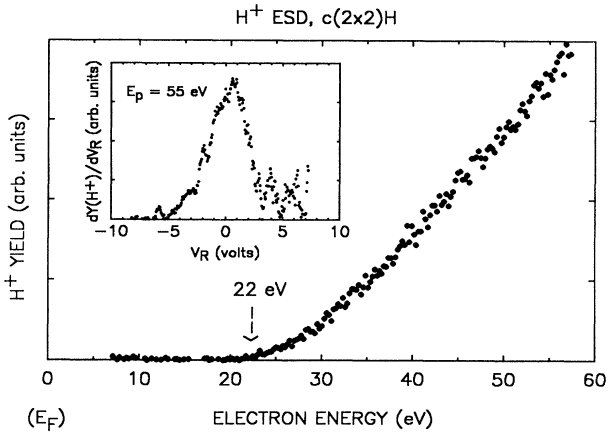

FIG. 10. ESD data (H^+ ion yield vs electron energy, referenced to the Fermi level) for the H-exposed $c(2\times2)$ surface ["$c(2\times2)H$"]. The desorption threshold of 22 eV is indicated. The inset shows the H^+ kinetic-energy distribution for an incident electron energy of 55 eV. V_R is the sample bias with respect to ground (see text), and the quantity plotted is the derivative of the ion yield, $Y(H^+)$, with respect to V_R. More energetic ions correspond to more negative values of V_R.

The H^+ desorption threshold of 22 eV suggests that the H is adsorbed on saturated C sites (i.e., sp^3- as opposed to sp^2-hybridized C). H^+ thresholds of ≈23–25 eV are observed[33] for molecules such as $(CH_3)_4C$ and $(CH_3)_4Si$ in the condensed phase, whereas C_6H_6 gives[33] an H^+ onset at about 29 eV. However, there are insufficient H^+ ESD data for other condensed unsaturated hydrocarbons to permit complete confidence in this interpretation of the threshold energy. Before exposure of the $c(2\times2)$ surfaces to H, the H^+ ESD was barely above the noise level. This indicates that, given the high SiC temperatures (≈1100 °C) during C_2H_4 exposure, no H remains on the surface. This is consistent with data for C_2H_4 adsorbed on Si(111) (Ref. 34) or Si(001) (Ref. 35) which show that dehydrogenation is complete by about 500 °C.

F. The thermally generated $c(2\times2)$ surface

Although the work described above has focused primarily on C adsorption on the Si-terminated surface, some results were also obtained for the thermally generated $c(2\times2)$ structure formed by annealing the (2×1) surface in UHV for several minutes at about 1250 °C. Most significant is the fact that the C 1s ELS (not shown) closely resembles that for the C_2H_4-derived $c(2\times2)$ in Fig. 6 with, in some cases, superimposed weak graphitic features corresponding to the (1×1) structure. As noted above, formation of the $c(2\times2)$ surface by thermal desorption of Si is generally accompanied by production of some graphitic C. The fractional-order spots in the thermal $c(2\times2)$ are generally less sharp and bright than those for the C_2H_4-derived $c(2\times2)$ and the I(C)/I(Si) PPH ratio more variable. A series of atomic H experiments, similar to those discussed above, were performed for the thermal $c(2\times2)$. The results were in all respects essentially identical to those shown in Figs. 8 and 9.

These observations suggest that the structure and chemical bonding are the same in either case but that the C_2H_4-derived $c(2\times2)$ is more homogeneous (i.e., graphite-free) and the ordering more nearly complete.

G. Model for high-temperature C_2H_4 adsorption

The data discussed above are all consistent with a C_2H_4 reaction which leaves the C—C σ bond intact while forming Si—C σ bonds between the Si termination layer of the substrate and the adsorbed C. For the purpose of the present discussion these will be termed

" $>C—C<$ bridges." The C hybridization in this model is sp^3 which leaves one dangling bond per adsorbed C. All Si atoms are fully fourfold coordinated in this structure. For the thermally generated $c(2\times2)$, the proposed structure would arise naturally when Si is desorbed from the (2×1) termination layer and the remaining C atoms form σ-bonded pairs to eliminate one of the two dangling bonds per C.

Figure 11 shows a model for the $c(2\times2)$ surface in which $>C—C<$ bridges form between alternating pairs of surface Si atoms in staggered rows, giving a C coverage equivalent to one monolayer. The (1×2) structure which is formed, with no change in C coverage, by annealing the $c(2\times2)$ surface in UHV requires a different arrangement. The $c(2\times2)\rightarrow(1\times2)$ transformation could occur by "unstaggering" the rows of bridges, as indicated in Fig. 11. The (1×2) structure also occurs (Figs. 1 and 4), prior to the onset of the $c(2\times2)$ phase, with increasing C_2H_4 exposure. As noted above, the (1×2) fractional-order spots are always weak and diffuse in contrast to those for (2×1) and $c(2\times2)$. This suggests that the (1×2) ordering is unstable and confined to relatively small areas of the surface. The proposed $c(2\times2)$ structure resembles the staggered-dimer model suggested by Dayan,[27,36] except that Dayan assumed Si termination for this surface. However, more recent work,[3,6] together with the present results, indicates C termination.

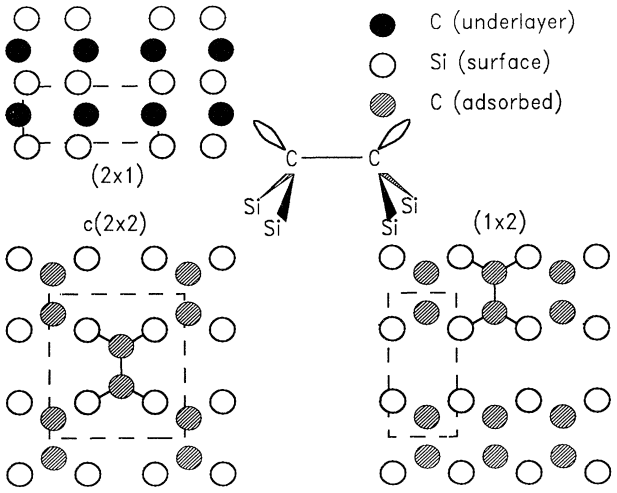

FIG. 11. Schematic diagram of different β-SiC(001) surface structures. The clean (2×1) surface is shown with the underlayer C atoms in the bulk lattice positions and the surface Si atoms displaced to form dimer pairs. For the $c(2\times2)$ and (1×2) surfaces, Si atoms are shown in the bulk lattice positions with the adsorbed C forming bridges (underlayer C atoms not shown). The dashed lines show the unit cells, with that for $c(2\times2)$ being nonprimitive. Atom sizes and distances are not to scale. Also shown is the proposed structure for a C-dimer bridge. The ellipsoids represent the C sp^3 dangling bonds on the H-free surface. The $c(2\times2)$ and (1×2) diagrams also indicate the orientation of the bridging bonds with respect to the surface Si atoms.

The proposed model is different from the di-σ structure suggested[34,35] on the basis of LEED and vibrational electron-energy-loss spectroscopy for C_2H_4 adsorption on Si(001) and Si(111) at low temperature. In that model, $—CH_2—CH_2—$ units form the bridges. The Si(001)-(2×1) LEED symmetry is unaffected by C_2H_4 chemisorption,[35] indicating that the bridges take the place of the dimer pairing on the clean surface. [Interestingly, one group[37] has studied the low-temperature adsorption of C_2H_4 on cleaved Si(111)-(2×1) surfaces and found evidence for a π-donor–π^*-acceptor complex with a weakened $H_2C=CH_2$ bond.] The results described above for adsorption of atomic H on the SiC $c(2\times2)$ surface indicate that the analogous species, a $>CH—CH<$ bridge, can also be formed. This is shown by the complete, but thermally reversible, removal of the C dangling-bond features from the C 1*s* ELS and C *KLL* AES.

It is useful to estimate bond angles for the proposed bridge structure as a qualitative indicator of strain. For SiC(001), the Si-Si nearest-neighbor distance on the unreconstructed surface is 3.08 Å. We assume a surface Si—C bond length equal to the bulk value of 1.89 Å and a C-C distance of 1.54 Å (as in a typical saturated hydrocarbon). The computed Si-C-C and Si-C-Si angles are 114° and 109°, respectively, versus the ideal sp^3 value of 109.5°. Thus, the bridges can apparently form without a high degree of strain in the outermost layer. However, the structure as drawn in Fig. 11 does imply a torsion of the plane defined by the two Si-C backbonds at a given Si site relative to the plane of the two Si-C adsorbate bonds.

We have also considered several alternative structures. Leaving the C_2H_4 double bond intact while forming a bridge like that in Fig. 11 (i.e., $>C=C<$) would lead to a highly strained structure since the sp^2 hybridization of the C would require the bridge to lie nearly within the SiC surface plane. Si—C=C—Si bridges could replace dimer pairs on the clean (2×1) surface without severe bond-angle strain or the torsion required for the staggered dimer model in Fig. 11. However, the ELS data show evidence of a dangling C bond but not of the additional presence of either the C=C double bond or the one dangling bond per Si atom required in a $c(2\times2)$ structure based on such bridges at an adsorbed C coverage of one monolayer. Previous data[2] for the initial oxidation at room temperature of SiC(001)-(3×2), -(2×1), and -$c(2\times2)$ surfaces are also significant in this context. These results show that the process is dominated by formation of Si-O-Si bridges and that the $c(2\times2)$ is practically inert in comparison to the Si-terminated surfaces. This is further indirect evidence of the absence of reactive Si sites (i.e, dangling bonds) on the $c(2\times2)$ surface.

A Si-C-C-Si bridge, analogous to the di-σ bridge described above in connection with C_2H_4 on Si(001), is unlikely. The structure formed at 1100 °C is H-free and would, therefore, have an energetically unfavorable two dangling bonds per C with no apparent mechanism for pairing such bonds on different bridges. Finally, complete dissociation of the ethylene molecule to form Si-C-Si bridges is considered unlikely, again, because of the

two unpaired dangling bonds per C. Furthermore, such a structure should form easily during high-temperature exposure to CH_4 which is, in fact, found to be much less reactive than C_2H_4 under these conditions. Again, a $c(2\times2)$ structure based on either Si—C—C—Si or Si—C—Si bridges and an adsorbed carbon coverage of one monolayer would imply one dangling bond per Si atom in the outermost Si layer.

At this point we call attention to recent work by Powers *et al.*[38] on LEED I-V analysis of the thermal and ethylene-derived $c(2\times2)$ structures. These authors consider several different models (including the >C—C< bridge) and find that the Si—C=C—Si structure is most nearly consistent with LEED results. Although the data obtained in the present work (particularly the evidence for the absence of Si dangling bonds) are in better agreement with a model based on >C—C< bridges, it is not possible at present to decide with complete confidence between the two models. Other techniques giving structural information more directly could be applied here. Vibrational electron energy loss spectroscopy could distinguish between C—C and C=C bonds and could elucidate the C-H bonding on the H-saturated surface. H^+ electron stimulated desorption ion angular distribution (ESDIAD) data[39] could indicate the direction of the C—H bonds on the $c(2\times2)$H surface with respect to the single-domain (2×1) unit cell of the clean surface. Note the orientation of the C_2 pairs in Fig. 11. If a $c(2\times2)$ structure were formed by replacing Si-Si dimer pairs on the (2×1) surface with staggered rows of Si—C=C—Si bridges,[38] then the C—H bonds in the derived $c(2\times2)$H structure would lie in a plane at 90° with respect to those derived from the structure in Fig. 11.

Finally, we note that Matsunami *et al.*[40] have recently reported results for alternating exposures of β-SiC(001) to disilane (Si_2H_6) and to acetylene (C_2H_2) under conditions of temperature and pressure similar to those used here. Beginning with the (1×1) surface, reaction with Si_2H_6 leads first to the (2×1) structure, then to the (3×2). Subsequent exposure to C_2H_2 reverses this sequence. Evidently C_2H_2 and C_2H_4 behave very differently in that the former reacts with the (3×2) surface but does not produce a $c(2\times2)$ structure. Together, the present results and those in Ref. 40 indicate that *two* forms of C-terminated β-SiC(001) can be formed in a controlled manner by C adsorption. A "carbidic" $c(2\times2)$ structure can be prepared by reaction of the (2×1) surface with C_2H_4. A "graphitic" (1×1) structure can be prepared by reaction of the (2×1) or (3×2) surface with C_2H_2.

SUMMARY AND CONCLUSIONS

The formation of C-terminated β-SiC surfaces by the high-temperature reaction of C_2H_4 with SiC(001)-(2×1) surface has been studied with the following results.

(i) An exposure of about 50–70 L leads to a $c(2\times2)$ ordered monolayer of adsorbed C. Further C uptake is very slow.

(ii) Much larger exposures ($>10^3$ L) lead to a "graphitelike" (1×1) phase, recognizable by characteristic features in the C *KLL* Auger and in the valence and C 1*s* energy loss spectra.

(iii) Prolonged annealing of the $c(2\times2)$ at high temperature in UHV produces a poorly ordered (1×2) phase. The same phase also forms for small exposures ($\approx$10–40 L) of the initial (2×1) surface to C_2H_4.

(iv) The $c(2\times2)$ surface exhibits features in the C *KLL* Auger and C 1*s* energy-loss spectra which are associated with dangling C orbitals. These are removed by H adsorption and restored by thermal desorption of H. The H-saturated surface continues to exhibit a $c(2\times2)$ LEED pattern with, however, *I-V* characteristics somewhat different from those of the H-free surface. None of the data give any indication of dangling Si bonds on the $c(2\times2)$ surface.

(v) The SiC(001)-(3×2)Si ("excess-Si") surface is essentially inert to C_2H_4 under these conditions, and the SiC(001)-(2×1) surface reacts only slowly with CH_4 versus C_2H_4.

(vi) The $c(2\times2)$ surfaces formed by thermal desorption of Si from, and by reaction of C_2H_4 with, SiC(001)-(2×1) appear to be the same except that the latter is more uniform and well ordered.

(vii) A model for the $c(2\times2)$ carbon monolayer has been proposed which involves staggered rows of >C—C< units with sp^3-hybridized C atoms. Each carbon atom bridges two surface Si atoms, and each C has a single dangling bond on the H-free surface. All Si atoms in the outermost Si layer are fully fourfold coordinated.

Note added in proof. Since the submission of this work, two relevant papers have appeared. Ohshita[41] has performed *ab initio* molecular orbital calculations for adsorption of methylene (:CH_2) on SiC(001) and finds that the hollow bridge site between two Si atoms is energetically favored. Steffen *et al.*[42] have discussed the origin of the high-energy C *KLL* Auger satellite in ion-bombarded graphite in relation to defect formation.

ACKNOWLEDGMENTS

We are most grateful to L. Matus (NASA--Lewis Research Center) for providing the SiC samples and to J. M. Powers for extensive discussions, particularly with regard to structural models. We also thank D. E. Ramaker and B. I. Craig for helpful comments.

[1]R. Kaplan, Surf. Sci. **215**, 111 (1989).
[2]V. M. Bermudez, J. Appl. Phys. **66**, 6084 (1989).
[3]S. Hasegawa, S. Nakamura, N. Kawamoto, H. Kishibe, and Y. Mizokawa, Surf. Sci. **206**, L851 (1988).
[4]W. F. J. Slijkerman, A. E. M. J. Fischer, J. F. van der Veen, I. Ohdomari, S. Yoshida, and S. Misawa, J. Appl. Phys. **66**, 666 (1989).
[5]C.-S. Chang, N.-J. Zheng, I. S. T. Tsong, Y.-C. Wang, and R.

F. Davis, J. Am. Ceram. Soc. **73**, 3264 (1990); J. Vac. Sci. Technol. B **9**, 681 (1991).
[6]S. Hara, W. F. J. Slijkerman, J. F. van der Veen, I. Ohdomari, S. Misawa, E. Sakuma, and S. Yoshida, Surf. Sci. **231**, L196 (1990).
[7]B. I. Craig and P. V. Smith, Surf. Sci. **233**, 255 (1990).
[8]H. S. Kong, Y. C. Wang, J. T. Glass, and R. F. Davis, J. Mater. Res. **3**, 521 (1988).
[9]V. M. Bermudez and R. Kaplan, J. Mater. Res. **5**, 2882 (1990).
[10]V. M. Bermudez, T. M. Parrill and R. Kaplan, Surf. Sci. **173**, 234 (1986).
[11]M. J. Bozack, M. J. Dresser, W. J. Choyke, P. A. Taylor, and J. T. Yates, Jr., Surf. Sci. **184**, L332 (1987).
[12]E. L. Kern, D. W. Hamill, H. W. Deem, and H. D. Sheets, in Proceedings of the International Conference on Silicon Carbide, 1968, edited by H. K. Henisch and R. Roy [Mater. Res. Bull. **4**, S25 (1969)].
[13]D. R. Jennison, Phys. Rev. Lett. **40**, 807 (1978); P. J. Feibelman and E. J. McGuire, Phys. Rev. B **17**, 690 (1978).
[14]V. V. Khvostov, M. B. Guseva, V. G. Babaev, and O. Yu. Rylova, Surf. Sci. **169**, L253 (1986).
[15]D. E. Ramaker, J. Vac. Sci. Technol. A **7**, 1614 (1989).
[16]Y. Wang, R. W. Hoffman, and J. C. Agnus, J. Vac. Sci. Technol. A **8**, 2226 (1990).
[17]L. Papagano and L. S. Caputi, Surf. Sci. **125**, 530 (1983).
[18]A. Koma and K. Miki, Appl. Phys. A **34**, 35 (1984).
[19]S. V. Pepper, Surf. Sci. **123**, 47 (1982).
[20]D. Wesner, S. Krummacher, R. Carr, T. K. Sham, M. Strongin, W. Eberhardt, S. L. Weng, G. Williams, M. Howells, F. Kampas, S. Heald, and F. W. Smith, Phys. Rev. B **28**, 2152 (1983).
[21]J. F. Morar, F. J. Himpsel, G. Hollinger, J. L. Jordan, G. Hughes, and F. R. McFeely, Phys. Rev. B **33**, 1346 (1986).
[22]D. N. Belton and S. J. Schmieg, J. Vac. Sci. Technol. A **8**, 2353 (1990).
[23]V. M. Bermudez, J. Appl. Phys. **63**, 4951 (1988).
[24]J. F. Morar, F. J. Himpsel, G. Hollinger, J. L. Jordan, G. Hughes, and F. R. McFeely, Phys. Rev. B **33**, 1340 (1986).
[25]B. B. Pate, M. Oshima, J. A. Silberman, G. Rossi, I. Lindau, and W. E. Spicer, J. Vac. Sci. Technol. A **2**, 957 (1984).
[26]J. F. Morar, F. J. Himpsel, G. Hollinger, G. Hughes, and J. L. Jordan, Phys. Rev. Lett. **54**, 1960 (1985).
[27]M. Dayan, J. Vac. Sci. Technol. A **4**, 38 (1986).
[28]Y. Li and P. J. Lin-Chung, Phys. Rev. B **36**, 1130 (1987).
[29]A. Koma and R. Ludeke, Phys. Rev. Lett. **35**, 107 (1975).
[30]H. H. Madden, D. R. Jennison, M. M. Traum, G. Margaritondo, and N. G. Stoffel, Phys. Rev. B **26**, 896 (1982).
[31]J. A. Kelber, R. R. Daniels, M. Turowski, G. Margaritondo, N. H. Tolk, and J. S. Kraus, Phys. Rev. B **30**, 4748 (1984).
[32]C. F. Corallo, D. A. Asbury, M. A. Pipkin, T. J. Anderson, and G. B. Hoflund, Thin Solid Films **139**, 299 (1986).
[33]J. A. Kelber and M. L. Knotek, Surf. Sci. **121**, L499 (1982); J. Vac. Sci. Technol. A **1**, 1149 (1983).
[34]H. Froitzheim, U. Köhler, and H. Lammering, J. Phys. C **19**, 2767 (1986).
[35]J. Yoshinobu, H. Tsuda, M. Onchi, and M. Nishijima, J. Chem. Phys. **87**, 7332 (1987).
[36]M. Dayan, J. Vac. Sci. Technol. A **3**, 361 (1985).
[37]M. N. Piancastelli, M. K. Kelly, D. G. Kilday, G. Margaritondo, D. J. Frankel, and G. J. Lapeyre, Phys. Rev. B **35**, 1461 (1987).
[38]J. M. Powers, A. Wander, P. J. Rous, M. A. Van Hove, and G. A. Somorjai, Phys. Rev. B **44**, 11 159 (1991).
[39]R. D. Ramsier and J. T. Yates Jr., Surf. Sci. Rep. **12**, 243 (1991).
[40]H. Matsunami, M. Nakayama, T. Yoshinobu, H. Shiomi, and T. Fuyuki, in *Amorphous and Crystalline Silicon Carbide and Related Materials II,* edited by M. M. Rahman, C. Y.-W. Yang, and G. L. Harris, Springer Proceedings in Physics Vol. 43 (Springer, Berlin, 1989), p. 157.
[41]Y. Ohshita, J. Cryst. Growth **110**, 516 (1991).
[42]H. J. Steffen, C. D. Roux, D. Marton, and J. W. Rabalais, Phys. Rev. B **44**, 3981 (1991).

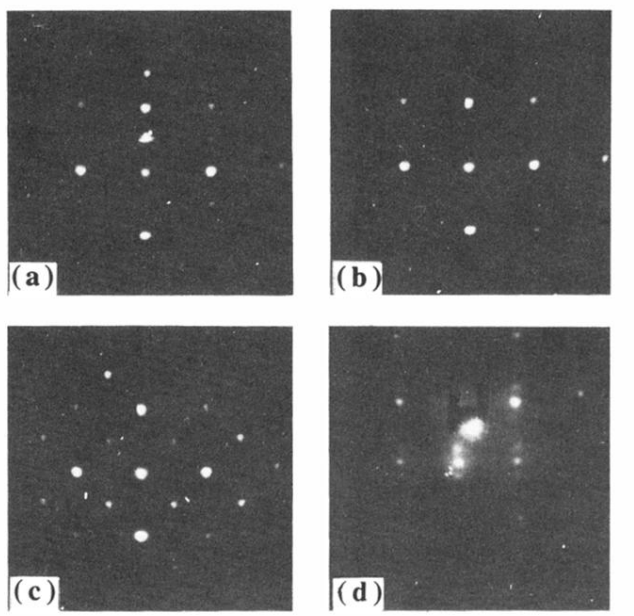

FIG. 1. LEED patterns for (a) (2×1), (b) (1×2), (c) $c(2\times2)$, and (d) (1×1) single-domain β-SiC(001) surfaces. Data were obtained at a primary beam energy of 99 eV except for the (1×1) which was obtained at 116 eV.